


## Sequential resonance for giant quantum oscillations above the energy barrier and its classical counterpart

Seiji Miyashita<sup>1,2,\*</sup> and Bernard Barbara<sup>3,†</sup>

<sup>1</sup>*JSR-UTokyo Collaboration Hub, CURIE, Department of Physics, The University of Tokyo, 113-0033, Hongo, Bunkyo-ku, Tokyo, 113-0033, Japan*

<sup>2</sup>*The Physical Society of Japan, 2-31-22, Yushima, Bunkyo-ku, Tokyo, 113-0034, Japan*

<sup>3</sup>*Institut Néel, CNRS/UGA, UPR2940 25 Avenue des Martyrs, BP 166, 38042 Grenoble Cedex 09, France*

 (Received 17 December 2023; revised 5 February 2024; accepted 8 February 2024; published 1 March 2024)

It has recently been shown that giant quantum oscillations above the energy barrier (GQOAB) of a spin  $S$  can be coherently induced by the simultaneous application of  $2S$  alternating fields (shaped field) associated with successive level separations [*Phys. Rev. Lett.* **131**, 066701 (2023)]. We begin the present paper with a more detailed study of the properties of GQOAB, such as the dependence of their frequency on the value of the anisotropy constant or on that of the amplitude of the alternating fields. We then extend the concept of GQOAB to the case where these ac-fields are applied, not simultaneously, but sequentially, showing that such a protocol also leads to coherent GQOAB but with a number of differences that are discussed in detail. We conclude with a classical approach of this problem showing that “giant classical oscillations above the barrier (GCOAB)” can also be designed at zero Kelvin.

DOI: [10.1103/PhysRevB.109.104301](https://doi.org/10.1103/PhysRevB.109.104301)

### I. INTRODUCTION

Passing through an energy barrier by quantum tunneling is one of the most remarkable topics of physics since the beginning of quantum mechanics [1–7]. The particular case of magnetism, with spin quantum tunneling, as in the quantum Stoner-Wohlfarth model [8], became increasingly important during the last decades with, in particular, the rise of mesoscopic magnetism (see the reviews in Refs. [9–11]). At the beginning, in the mid-1970s, mesoscopic quantum tunneling possibilities were pointed out in various nanoscale systems which focused on the quantum depinning of a domain wall trapped by nonmagnetic defects [12–15], and then on the tunneling of a single nanoparticle magnetic moment trapped by a magnetocrystalline anisotropy barrier [16–20]. This was also completed by a model describing the tunneling reversal of the magnetic moments of an antiferromagnetic nanoparticle [21].

More recently, it has been possible to extend these works to a more specific class of nanoparticles: The single molecules magnets (SMM) [22–27], and later to the rare-earth ions magnets (REM, consisting of uniaxial rare-earth ions, without or with nuclear spins, highly diluted in a nonmagnetic matrix) [28,29]. These systems exhibit the typical and fascinating stepwise hysteresis loop firstly observed on Mn12-ac [22] showing how mesoscopic quantum tunneling can reflect spin quantization, even in the presence of hysteresis (curious readers should also take a look at the reference [14] with magnetic avalanches induced by local spins tunneling in a much more complex system with no apparent quantization). In addition to their fundamental character, there is no doubt

that stepwise hysteresis loops of the Mn12-ac type should have applications in quantum information. In fact, qubit or multiqubit manipulation already considered in uniaxial magnetic systems with an energy barrier are always limited to a single potential well. In the rare cases where these ones were carried out on both sides of the barrier, it is with the tunneling effect and all its inconveniences (coincidence of states etc.) [30,31]. Regarding integrations, the blending of electro-nuclear spins for qubits and quantum circuits has been achieved [32–37], and numerous error correction quantum algorithms have been suggested [30,38–41]. In particular the multibits spins manipulations [42] involve quantum states connection through the creation/annihilation of the ladder operators, as in our approach, but also in the absence of a barrier which greatly reduces the possibilities of manipulation, as mentioned just above. And in the presence of an energy barrier, the entanglements are restricted to the pair of states which are in coincidence.

We have previously shown [43] that the application of a “shaped” field [44], which corresponds to the sum of all alternating fields of frequencies equal to each inter-state energy difference, enables transfer between states on either side of the barrier, just like the tunneling effect. Indeed, like the tunnel effect, this is a global resonance passing across the barrier, enabling states on either side of the barrier to be connected, but with one important difference: The levels do not have to be resonant. Although the intermediary oscillation between each pair of consecutive levels is a Rabi oscillation, the resulting oscillation passing over the barrier is not at all equivalent to a Rabi oscillation. We called it giant quantum oscillations above the barrier (GQOAB).

Such over-the-barrier quantum oscillations are an extension of Rabi oscillation to magnetic systems with uniaxial anisotropy and therefore with an energy barrier. This makes possible to manipulate complex superpositions of spin states

\*miyashita-seiji@g.ecc.u-tokyo.ac.jp

†bernard.barbara@neel.cnrs.fr

on each side of the barrier without having to apply a static transverse field and without the levels having to be in coincidence (i.e., without invoking the quantum tunneling effect). Beyond the possible applications in terms of multiqubits, the impact of this result touches on fundamentals of magnetism, which has always taught that only thermal activation or quantum tunneling can allow a spin to cross an energy barrier.

In this article, after a brief review of the model and method, we study in detail the dependence of the GQOAB [43] with the value of the applied ac-field and the anisotropy constant. Then we extend our concept of giant oscillations to the case where alternating fields are not applied simultaneously according to a given shaped field, but sequentially: A  $\pi$ -pulse corresponding to each level separation is applied successively from one pair of states to the next one. Such a protocol also leads to coherent GQOAB, but with a number of differences that are discussed in detail. For example, the sequential method requires a very precise control of the duration of each pulse to reverse the magnetization, which has important implications for the population dynamics of the other levels.

Finally, when the spin  $S$  tends to infinity, the GQOAB obtained by the application of a shaped field have a singularity, whereas those obtained by unbounded sequential  $\pi$  pulses have a classical limit. This led us to investigate the possibility of obtaining classical oscillations above the barrier. To do this, we started from the classical equations of motion of a spin [45] in the presence of an alternating field whose frequency evolves over time, as the limiting case of the sequential method when the level separation becomes infinitesimally small. Doing so, we were able to observe classical spin oscillations above the barrier that are very similar to GQOAB that we call “giant classical oscillations above the barrier (GCOAB).”

To sum up, this paper consists of four parts. After an introduction on giant quantum oscillations above the barrier [43] (Sec. I), Sec. II relates to the models and methods, while the dependencies of GQOAB are studied (i) on the different parameters of the problem in Sec. III and (ii) on other ac-fields excitations protocols in Sec. IV. In Sec. V we discuss the operations for the transfer between states. In Sec. VI, we develop the classical version of GQOAB, that we called GCOAB. The conclusion and last discussions are given in Sec. VII.

## II. MODEL AND METHOD

It is well known that the Hamiltonian of a spin  $S$  in the presence of an anisotropy energy barrier  $DS_z^2$ ,

$$\mathcal{H} = -DS_z^2 - H_z S_z, \quad S_z = S, S-1, \dots, -S, \quad (1)$$

has  $2S + 1$  states of energies:

$$E_m = -Dm^2 - H_z m, \quad m = S, S-1, \dots, -S. \quad (2)$$

In our recent paper [43], we started with an extension of this Hamiltonian in which we added a set of circularly polarized fields with frequencies equal to the energy differences:

$$\omega_{m \rightarrow m-1} = E_{m-1} - E_m = H_z + D(2m-1), \quad (3)$$

for the consecutive levels  $m$  and  $m-1$  of Eq. (1). In this case, the Hamiltonian is written

$$\mathcal{H} = -DS_z^2 - H_z S_z - h \left( \sum_{m=S}^{-S+1} \sin(\omega_{m \rightarrow m-1} t) S_x + \sum_{m=S}^{-S+1} \cos(\omega_{m \rightarrow m-1} t) S_y \right). \quad (4)$$

Note that if, with  $H_z = 0$  and only the first ac-field ( $m = S$ ) is applied, oscillations occur between  $S$  and  $S-1$ . Then, with a transverse field and depending on the helicity of this ac-field, the tunneling between the first excited states of one of the two wells, will be enhanced. This was achieved experimentally with the Fe<sub>8</sub> single molecule magnet [46].

The corresponding Schrödinger equation in the rotating frame, where

$$\Psi(t) = e^{i\omega S_z t} \Phi(t) \quad (5)$$

is given by

$$i\hbar \frac{\partial}{\partial t} |\Phi(t)\rangle = \left( -DS_z^2 - h_{ac} \frac{f(t)}{2i} (S^+ - S^-) \right) |\Phi(t)\rangle. \quad (6)$$

The sum of ac-fields in Eq. (4) can be written in terms of the shaped function [43]:

$$f(t) = \frac{\sin(2DS_t)}{\sin(Dt)}. \quad (7)$$

Starting from this Hamiltonian, it was found that the  $z$  component of spin  $S_z$  oscillates between the  $S$  and  $-S$  states, passing over the barrier and leading to what we called “giant quantum oscillations above the barrier (GQOAB)” [43]. A specific property of this Hamiltonian is that the motion of  $S_z$  does not depend on  $H_z$ .

Clearly, this motion is very different from the usual Rabi oscillations (occurring when  $D = 0$ ), the Hamiltonian of which in the normal frame, with  $\omega = H_z$ , is written

$$\mathcal{H}_{\text{Rabi}} = -H_z S_z - h_{ac} (\sin(\omega t) S_x + \cos(\omega t) S_y). \quad (8)$$

In this case, the magnetization rotates around the  $z$  axis with the frequency  $\omega = H_z$  and  $M_z$  changes sinusoidally around the  $y$  axis with the period:

$$T = \frac{2\pi}{h_{ac}}. \quad (9)$$

## III. DEPENDENCIES OF GQOABS ON THEIR VARIOUS PARAMETERS

### A. Dependence on $h_{ac}$

Some aspects of the dependence of GQOAB on the ac-field amplitude  $h_{ac}$  were reported in the SM of our previous paper [43]. In particular, it was shown that the period of GQOAB is proportional to  $1/h_{ac}$ , if  $h_{ac}$  is not too small ( $h_{ac} > 0.005$ ). To illustrate this result, we show the GQOAB calculated for several values of  $h_{ac}$  as a function of the timescale  $t$  in Fig. 1(a). In Fig. 1(b), they are shown as a function of  $t \times h_{ac}$  and in this case, all the curves collapse in a single one proving that the time dependence of GQOAB is a function of the product  $t \times h_{ac}$ , and therefore that the period of GQOAB is proportional to  $1/h_{ac}$ .

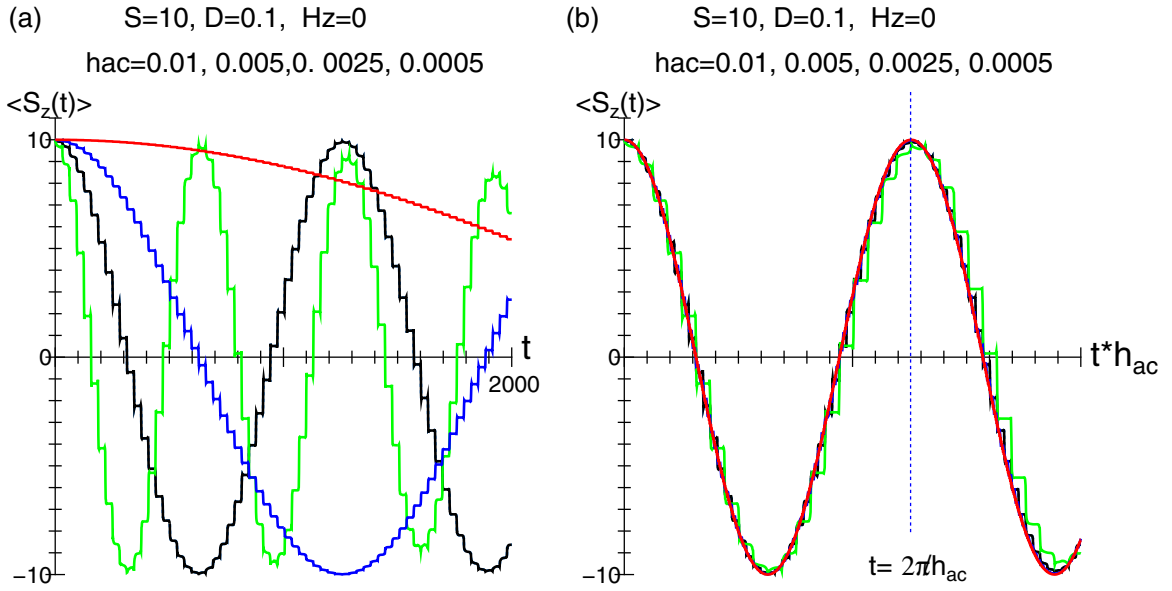


FIG. 1.  $h_{ac}$ -dependence of  $S_z(t)$ .  $h_{ac} = 0.01$  (green),  $0.005$  (black),  $0.0025$  (blue), and  $0.0005$  (red). (a)  $S_z(t)$  as a function of  $t$ . (b)  $S_z(t)$  as a function of the scaled time  $t \times h_{ac}$ .

However, for larger  $h_{ac}$ , a stepwise structure, more perceptible (blue, black, and green curves in Fig. 1), superimposes on the GQOAB sinusoidal curve (red curve in Fig. 1). Clearly, such a steplike structure reflects the individual oscillations taking place between successive levels. In addition, the spin fidelity (classical length of magnetization),

$$s_f = \langle S_x \rangle^2 + \langle S_y \rangle^2 + \langle S_z \rangle^2, \quad (10)$$

is not constant as shown by its oscillations in Fig. 2, which emphasizes the quantum nature of GQOAB, in opposition to Rabi oscillations where the length of the spin remains constant ( $s_f$  is constant).

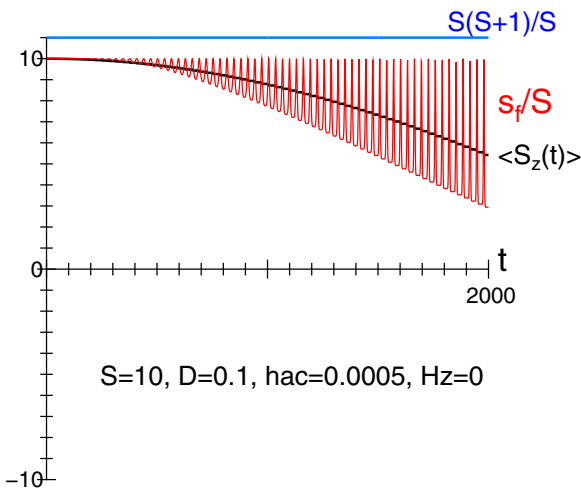


FIG. 2. Initial motion of  $\langle S_z(t) \rangle$  (bold black curve) for  $S = 10$ ,  $H_z = 0.0$ , and  $h_{ac} = 0.0005$ . The classical spin length (spin-fidelity  $s_f/S$ ) is given by the thin red curve and the normalized quantum spin-size  $S(S + 1)/S$  is given by the blue line.

## B. Dependence on the anisotropy constant $D$

In this section, we will try to see if it is possible to find a continuous evolution of GQOAB (finite anisotropy  $D$ ) towards Rabi oscillations ( $D = 0$ ). In fact, we found that near  $D = 0$  the evolution of GQOAB is rather tricky. Let us start with the case of a typical GQOAB where each applied ac-field has a frequency equal to the energy difference between successive spin levels. In this case the successive operations such as  $\omega_{m \rightarrow m-1}$  and  $\omega_{m-1 \rightarrow m-2}$  can act almost independently because their energy difference  $\omega_{m \rightarrow m-1} - \omega_{m-1 \rightarrow m-2} = 2D$  is large enough. The steplike structure of Figs. 3(a) and 3(b) is no longer visible in Fig. 3(c). Setting  $Dt = \tau$  in the rotating frame expression (6), the equation of motion becomes

$$i\hbar \frac{\partial}{\partial \tau} |\Phi(t)\rangle = \left( -S_z^2 - \frac{h_{ac}}{D} f(\tau/D) S_y \right) |\Phi(t)\rangle, \quad (11)$$

$$f(\tau/D) = \frac{\sin(2S\tau)}{\sin \tau},$$

where  $\tau = Dt$ . Because  $f(\tau/D)$  is independent of  $D$ , this form indicates that the period of GQOAB oscillations is proportional to the amplitude  $1/(h_{ac}/D)$  in the time scale  $\tau = Dt$ . That is, in the original time scale  $t$ , the period does not depend on  $D$ , i.e.,

$$T_{\text{period}} = 2\pi \frac{1}{D} \frac{1}{(h_{ac}/D)} = \frac{2\pi}{h_{ac}}, \quad (12)$$

showing that the GQOAB period is independent of  $D$  and that, in spite of their basic differences, GQOAB and the two-levels Rabi oscillations have the same period  $2\pi/h_{ac}$ .

The resonance frequencies  $\omega_{m \rightarrow m-1}$  for different  $m$  being quite different when  $D$  is large [see Eq. (12)], the duration for the transitions between neighboring states ( $m \rightarrow m-1$ ) should not depend on  $D$  [see Eqs. (8) and (9)]. In this case, the operations with the resonance frequencies work almost independently, and the GQOAB are almost independent of  $D$ .

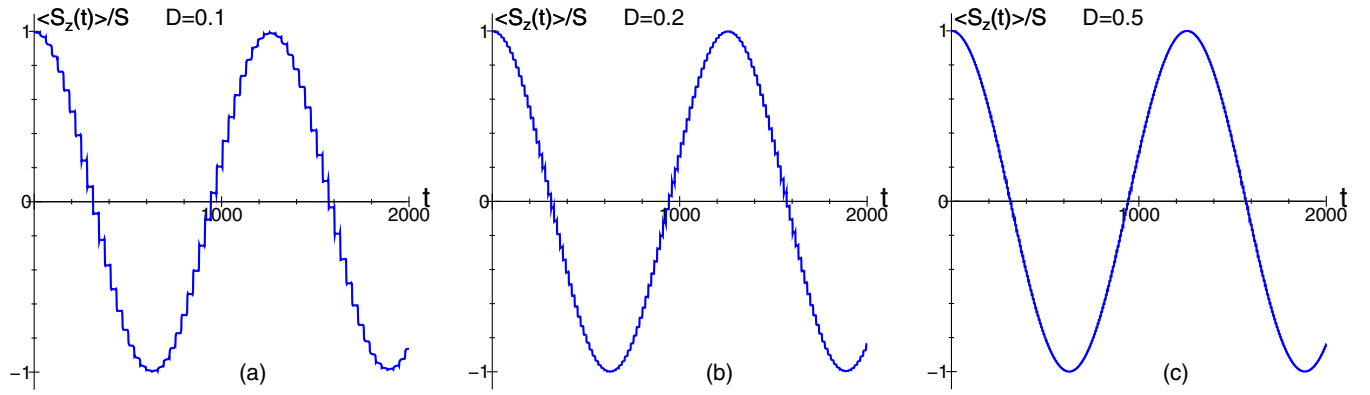


FIG. 3.  $D$ -dependence of  $S_z(t)/S$  with  $H_z = 0.0$  and  $h_{ac} = 0.005$ . (a)  $D = 0.1$ , (b)  $D = 0.2$ , (c)  $D = 0.5$ . The initial state is  $(S_x, S_y, S_z) = (0, 0, 1)$ .

Regarding possible applications, this is an interesting point, because any spin system can do the trick whatever the value of the anisotropy constant  $D$  and therefore whatever the height of the barrier  $DS^2$  (1) as long as the spin is not too large (see below).

However, this is no more the case when  $D$  becomes very small ( $D = 0.001, \dots, 0.05$ ) and therefore this energy difference becomes smaller. In this case, the main periods remain the same (Fig. 4) because (12) is independent of  $D$ , but the shapes of  $\langle S_z(t) \rangle$  change largely: As the anisotropy constant  $D$  becomes smaller, the successive resonance frequencies become closer to each other, and therefore interfere more, increasingly disrupting the spin inversion mechanism that causes GQOAB. This leads to the stepwise oscillations of Fig. 4.

In the limit  $D = 0$ ,  $H_z \neq 0$ , the  $2S$  terms of the sum over  $m$  in Eq. (4) with  $\omega_{m \rightarrow m-1}$  (3) have the same value, and thus the amplitude of their sum becomes  $2S$  times larger. The system comes back to the case of normal Rabi oscillations with  $2S$  times faster frequency, i.e., with period  $[2\pi/(2Sh_{ac})]$ . It should be noted that the period of GQOAB is  $2\pi/h_{ac}$  (12) regardless of  $D$ , but here, with  $D = 0$ , we find the period  $2\pi/(2Sh_{ac})$ , which is  $2S$  times faster.

To conclude this part, when  $D \rightarrow 0$ , the period of oscillations changes from the GQOAB one ( $2\pi/h_{ac}$ ) to the multi-Rabi one [ $2S$  times faster Rabi oscillations =  $2\pi/(2Sh_{ac})$ ],

and the dynamics becomes more complex in between as shown in Fig. 5.

For the cases with small  $D$ , e.g.,  $D = 0.02 \sim 0.0001$  in Fig. 5, irregular motions are observed. As shown in Eq. (11), if we scale the time by  $D$ . It should be noted that  $D$ -dependence appears only in the coefficient of  $S_y$ , where  $f(\tau/D)$  does not depend on  $D$ , but depends on  $S$  and  $\tau$ . Then, for small  $D$ , the coefficient  $h_{ac}f(\tau/D)/D$  becomes large, and the spin moves in a large complicated time dependent field, and the motion is not intuitively understood. As indicated in the next section, the long-term dynamics is an interesting problem, but its more detailed analysis is saved for a future study.

### C. Long-time behavior of GQOAB

Contrary to the exact sequence of exchange operation which will be studied in the next section, the GQOAB obtained from the application of all the required ac-fields (shaped function) does not lead to a perfect spin reversal due to an effect of the applied ac-fields on neighboring transitions. Although this effect is very small, it leads to a beating of GQOAB as depicted Fig. 6 [note that the GQOAB reversal shown in previous figures up to  $t = 2000$  (e.g., Fig. 5) corresponds to the first oscillation in Fig. 6]. During the long beating period, the classical spin length (spin-fidelity) (10)

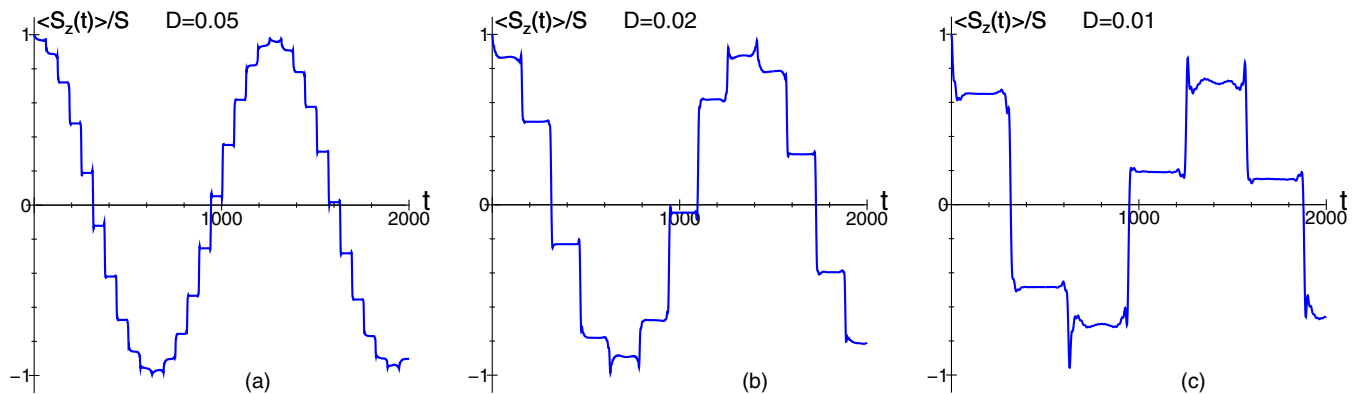


FIG. 4.  $D$ -dependence of the time dependence of  $S_z(t)/S$  with  $H_z = 0.0$  and  $h_{ac} = 0.005$ . (a)  $D = 0.05$ , (b)  $D = 0.02$ , (c)  $D = 0.01$ . The initial state is  $(S_x, S_y, S_z) = (0, 0, 1)$ .

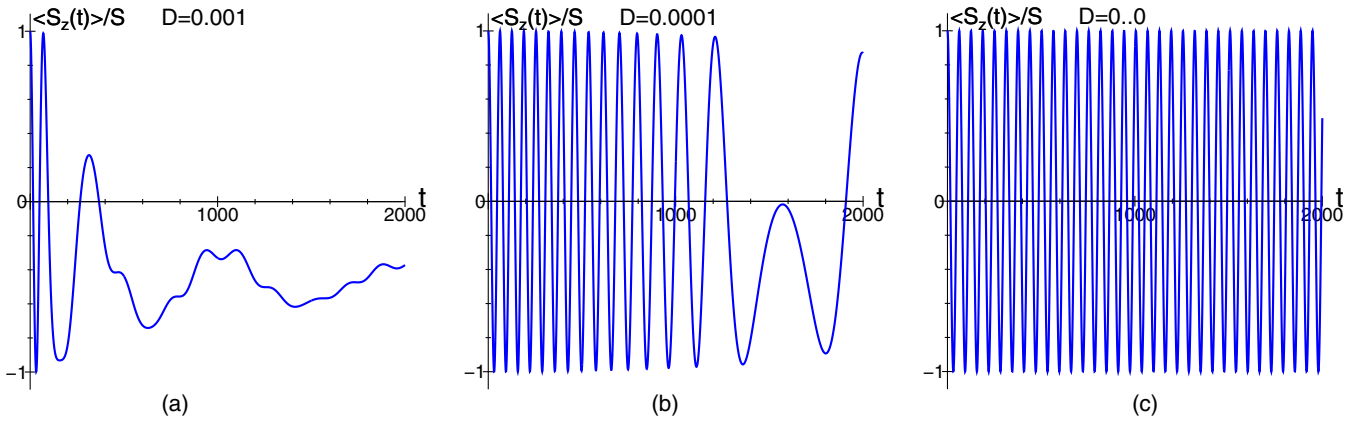


FIG. 5.  $D$ -dependence of the of  $S_z(t)/S$  oscillations for the example  $H_z = 0$  and  $h_{ac} = 0.005$ , showing the continuous passage from an intermediate noisy regime to the Rabi regime. (a)  $D = 0.001$ , (b)  $D = 0.0001$ , (c)  $D = 0$  (same as Rabi-oscillation with  $h_{ac} = 0.005 \times 20$ ). The initial state is  $(S_x, S_y, S_z) = (0, 0, 1)$ .

also shows a beating while the value of  $\langle S^2 \rangle$ ,

$$S(S+1) = \langle S_x(t)^2 \rangle + \langle S_y(t)^2 \rangle + \langle S_z(t)^2 \rangle, \quad (13)$$

is always conserved. In a rotation of the spin vector like the usual classical Rabi-oscillation, both of them are conserved:

$$s_f = S^2, \quad \langle S^2 \rangle = S(S+1). \quad (14)$$

It should be noted that if and only if all the levels separations are the same (which is never the case in the presence of an anisotropy), there is no beating [Fig. 5(c)], and this is because, in this case, the oscillations are simple Rabi oscillations.

#### IV. PROTOCOL FOR SUCCESSIVE TRANSFER OPERATIONS

In this section, we take a step further in explaining the way the GQOAB are induced: Instead of applying all the frequencies at the same time (shaped field), we shall use a sequential application of  $\pi$ -pulses with the frequencies  $\omega_{m \rightarrow m-1}$  equal to the successive energy levels  $m = S, S-1, \dots, S+1$ .

##### A. Resonant transitions between two states in a uniaxial spin system ( $S > 1/2$ ) with a resonance field (Resonance operation)

The effect of a single ac-field inducing the transition between states  $m$  and  $m-1$  is described, for  $H_z \neq 0$ , by the following Hamiltonian:

$$\begin{aligned} \mathcal{H}_{ac} &= -DS_z^2 - H_z S_z + \mathcal{H}_{ac\text{-field}}, \\ \mathcal{H}_{ac\text{-field}} &= -h_{ac}(\sin(\omega_{m \rightarrow m-1}t)S_x + \cos(\omega_{m \rightarrow m-1}t)S_y), \end{aligned} \quad (15)$$

which gives a good approximation for the pure two-level Rabi oscillation with an anisotropy term, as will be discussed in Sec. V A. It is clear that GQOAB can be considered as the superposition of such  $2S$  Rabi oscillations with different frequencies.

##### B. Transfer operation

From the previous section, it is clear that the operation  $e^{-i\mathcal{H}_{ac}t/\hbar}$  with  $\mathcal{H}_{ac}$  given by Eq. (15),

$$U(m, m-1, t) = e^{-i\mathcal{H}_{ac}t/\hbar}, \quad (16)$$

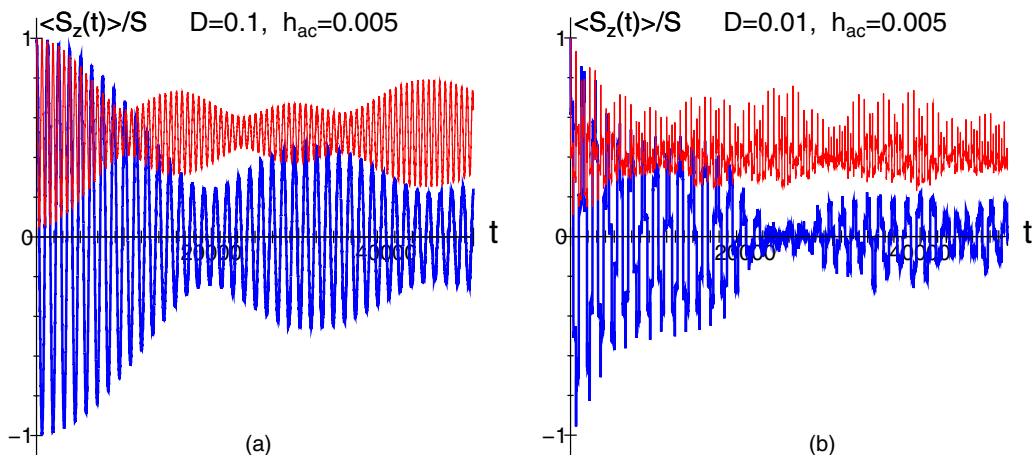


FIG. 6. Long-time behavior (up to  $t = 50000$ ) of  $S_z(t)/S$  (bold blue curve) under the application of the ac-field  $\omega_S, \dots, \omega_{-S+1}$  with  $h = 0.005$ . (a)  $D = 0.1$  and (b)  $D = 0.01$ . The spin-fidelity  $s_f$  is also plotted (thin red curve). The initial state is  $(S_x, S_y, S_z) = (0, 0, 1)$ .

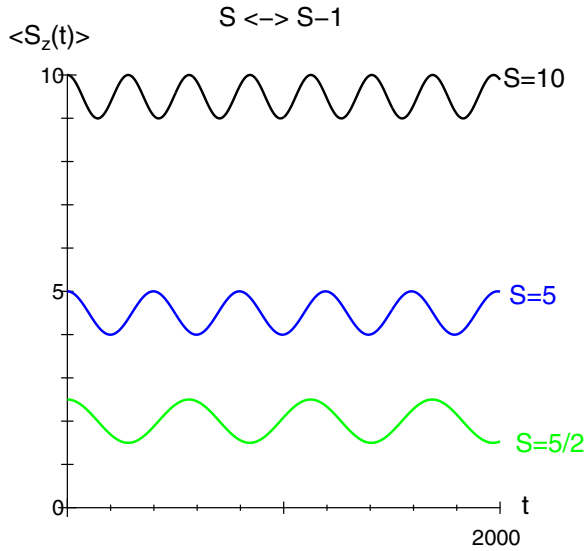


FIG. 7.  $S$  dependence of  $S_z(t)$  oscillations between  $S$  and  $S - 1$ .  $S = 10$  (black),  $S = 5$  (blue), and  $S = 5/2$  (green).

causes oscillations between the states of  $m$  and  $m - 1$ . Setting the time to be a half-period,

$$t = T/2 = \pi/h_{ac}, \quad T = 2\pi/h_{ac}, \quad (17)$$

the operation

$$X(m, m - 1) = U(m, m - 1, \pi/h_{ac}) = e^{-i\mathcal{H}_{ac}(\pi/h_{ac})/\hbar} \quad (18)$$

induces the transition between the states  $m$  and  $m - 1$ .

### C. Sequential operations and the GQOAB

When we successively apply the transfer operation (18), sequential transfer from  $|S\rangle$  to  $|S'\rangle$  takes place:

$$|S'\rangle = X(S' - 1, S') \cdots X(S - 1, S - 2)X(S, S - 1)|S\rangle. \quad (19)$$

This is a kind of sequence of gate operation in quantum computing. Even if it is not 100% precise, the operation  $X(m, m - 1)$  nevertheless gives a sufficiently precise transition between the specified pairs of levels.

The full reversal of magnetization, from  $S$  to  $-S$ , is given by the operations

$$|-S\rangle = X(-S + 1, -S) \cdots X(0, -1)X(1, 0) \cdots \\ \times X(S - 1, S - 2)X(S, S - 1)|S\rangle, \quad (20)$$

which leads to spin oscillations which are, at first sight, identical to GQOAB. First, we study the dependence of the period of the oscillation between  $S$  and  $S - 1$ . The ac-field  $h_{ac}$  being multiplied by  $\sqrt{2S}$  [see Eq. (30) below], the period of oscillation must be proportional to  $1/\sqrt{2S}$  as confirmed numerically (Fig. 7). Using the  $\pi$ -pulse operations (18), we can change the magnetization from  $S$  to  $S - 1$ , and the full operation (20) allows us to achieve the reversal from  $S$  to  $-S$ . Some results of these simulations are shown Fig. 8, where the oscillations are given for different values of the spin  $S$ . We might call these oscillations sequential quantum oscillations above the barrier (SQOAB).

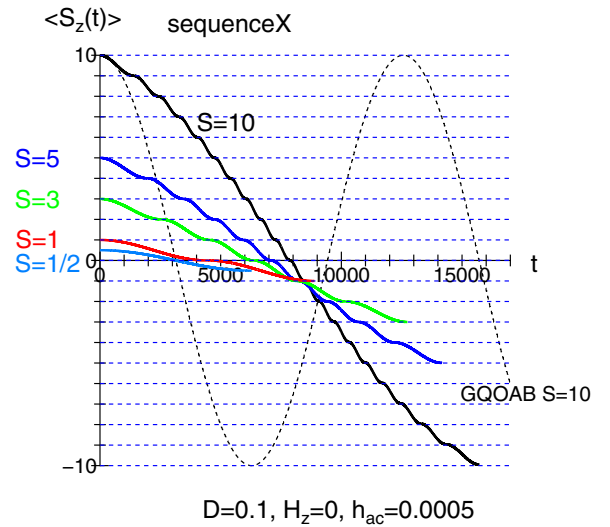


FIG. 8.  $S_z(t)$  obtained with the sequential operation (20) for  $S = 10, 5, 3$ , and  $1/2$  with  $h_{ac} = 0.0005$ . The short-dotted curve represents a GQOAB, with same parameters and  $S = 10$ .

Each step is given by a  $\pi$  pulse, the frequency of which is equal to the energy levels separation. The period of  $\pi$  pulse does not depend on the frequency and is proportional to the ac-field amplitude, as given by Eq. (9). Note that the ac-field amplitude for the step between  $S_z = m$  and  $m - 1$  is given by  $h_{ac}\sqrt{S(S+1) - m(m-1)}$ . Therefore, the period of each step is given by  $2\pi/h_{ac}\sqrt{S(S+1) - m(m-1)}$ , and the associated time  $t_{\text{reverse}}$  for the reversal (half of the period) of spin  $S$  becomes

$$t_{\text{reverse}}^{\text{SQOAB}} = \sum_{m=S}^{-S+1} \frac{\pi}{h_{ac}\sqrt{S(S+1) - m(m-1)}}, \quad (21)$$

which increases with  $S$  slowly. Thus, periods of steps are different, and their sum (21) is not  $\pi/h_{ac}$ , in contrast to the period of GQOAB is given nearly by

$$t_{\text{reverse}}^{\text{GQOAB}} \simeq \frac{\pi}{h_{ac}}. \quad (22)$$

### D. Comparison between GQOAB and SQOAB

As shown in our previous report [43], GQOAB are induced by the application of a shaped field (sum of all the interstates ac-fields between  $S$  and  $-S$ ), according to the Hamiltonian (4). In GQOAB, the reversal time  $t_{\text{reverse}}$  (22) of magnetization is almost independent of  $S$ .

Figure 8 shows clearly that GQOAB are faster than SQOAB and the reason for that is the following: In the sequential operation the ac-field of the next frequency is applied after the previous one finished, while in GQOAB all the frequencies are applied simultaneously.

For the wave function,

$$\Psi(t) = c_S(t)|S\rangle + c_{S-1}(t)|S-1\rangle + \cdots \\ + c_{1-S}(t)|1-S\rangle + c_{-S}(t)|-S\rangle, \quad (23)$$

the population of each state is given by

$$p(S_z) = |c_{S_z}(t)|^2. \quad (24)$$

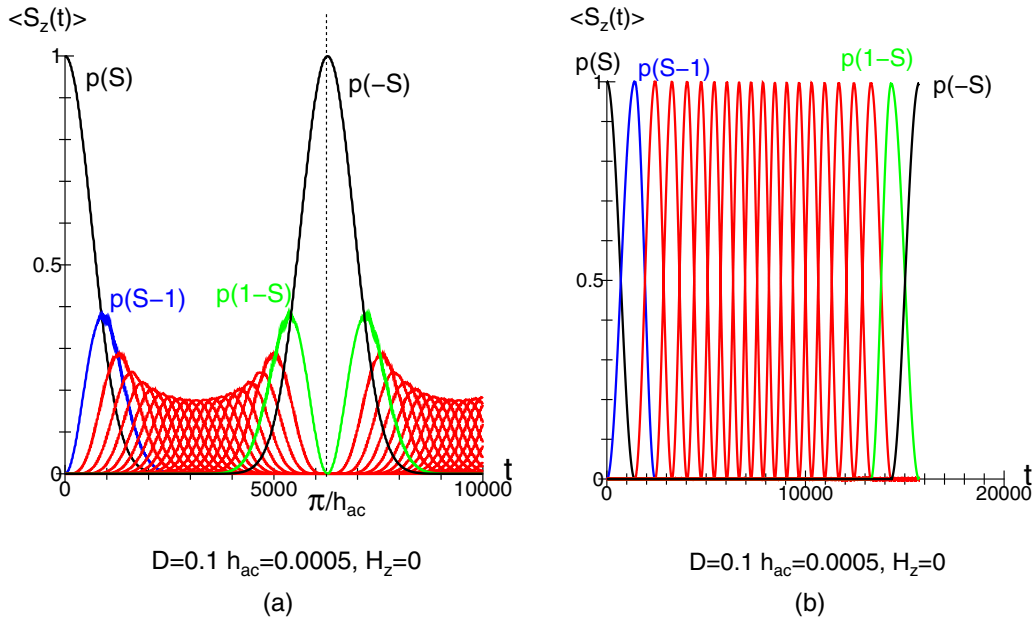


FIG. 9. (a) Time dependence of the population  $p(S_z)$ ,  $S_z = S, S - 1, \dots, 1 - S, -S$  ( $S = 10$ ) for GQOAB. (b) SQOAB process of  $X_s$ .  $D = 0.1$ ,  $H_z = 0.1$  with the amplitude  $h_{ac} = 0.005$ .

The time dependencies of populations  $p(S_z)$  of GQOAB and SQOAB are plotted Fig. 9. The most obvious difference between the two is the important overlaps of GQOAB, showing the coexistence of several states at a given instant (leaking). Such overlaps do not appear with SQOAB where the transitions occur one by one. Another difference is the predominance of the time occupancies of the large  $|M_z| (\simeq S)$  state components in GQOAB while all states occupancies are the same with SQOAB.

Although both operations give spin reversals above the barrier, the SQOAB procedure (20), in which the sequential application of the  $2S$  ac-fields is required to be precisely coordinated, causes technical difficulties in numerical calculations and experimental applications. Therefore, even if SQOAB is feasible, the application of the shaped field of GQOAB should be more practical for experimental realizations of spin reversal.

## V. OPERATIONS FOR THE TRANSFER BETWEEN THE STATES $m$ AND $m - 1$ EXPRESSED BY THE SPIN OPERATORS OF $S > 1/2$

Each operation for transfer between  $|m\rangle$  and  $|m - 1\rangle$  in GQOAB given by Eq. (15), is very close but not identical to the operation inducing pure Rabi oscillations between these two states. Indeed, Eq. (15) inevitably involves transfers to the off-resonant  $m - 2$  and  $m + 1$  states. In this section, the properties of operations for the transfer between the states  $m$  and  $m - 1$  expressed by the spin operators of  $S > 1/2$  are studied, and the exact formula inducing the pure Rabi oscillations is examined.

### A. Leaks to neighboring states

Neglecting minor off-resonant transitions involving  $m - 2$  and  $m + 1$ , we consider here only oscillations between  $m$  and

$m - 1$ . The corresponding matrix elements are given by the ladder operations:

$$\begin{aligned} S^+ |m\rangle &= \sqrt{S(S+1) - m(m+1)} |m+1\rangle, \\ S^- |m\rangle &= \sqrt{S(S+1) - m(m-1)} |m-1\rangle. \end{aligned} \quad (25)$$

To put it simply, let us consider the case  $m = S$ :

$$S^+ |S-1\rangle = \sqrt{2S} |S\rangle, \quad S^- |S\rangle = \sqrt{2S} |S-1\rangle. \quad (26)$$

Regarding the specified two states, we replace  $|S\rangle$  and  $|S-1\rangle$  by  $|+\rangle$  and  $|-\rangle$ , respectively, and we also introduce the modified ladder operators  $\sigma^+$  and  $\sigma^-$ :

$$\begin{aligned} S^+ &= \sqrt{2S} |S\rangle \langle S-1| \rightarrow \sqrt{2S} |+\rangle \langle -| = \sqrt{2S} \sigma^+, \\ S^- &= \sqrt{2S} |S-1\rangle \langle S| \rightarrow \sqrt{2S} |-\rangle \langle +| = \sqrt{2S} \sigma^-, \end{aligned} \quad (27)$$

and

$$S_z \simeq S + \frac{\sigma^z - 1}{2}, \quad (28)$$

because when  $\sigma = 1$ ,  $S_z = S$ , and when  $\sigma = -1$ ,  $S_z = S - 1$ . The spin operators are  $(2S + 1) \times (2S + 1)$  matrices which act on all the  $2S + 1$  states, while the operations given by  $\sigma$  are  $2 \times 2$  matrices which act on the two states  $|+\rangle$  and  $|-\rangle$ .

Noting that

$$\begin{aligned} \sin(\omega t) S_x + \cos(\omega t) S_y &= \frac{e^{i\omega t} - e^{-i\omega t}}{2i} \frac{S^+ + S^-}{2} \\ &\quad + \frac{e^{i\omega t} + e^{-i\omega t}}{2} \frac{S^+ - S^-}{2i} \\ &= \frac{e^{i\omega t} S^+ - e^{-i\omega t} S^-}{2i}, \end{aligned} \quad (29)$$

the Hamiltonian (1) is rewritten in terms of the operators ( $\sigma$ ) as

$$\begin{aligned} \mathcal{H}_{\text{two-level}} &= -H_z \left( S + \frac{\sigma^z - 1}{2} \right) - D \left( S + \frac{\sigma^z - 1}{2} \right)^2 \\ &\quad - \sqrt{2S} h_{ac} \left( \frac{e^{i\omega_S \rightarrow S-1t} \sigma^+ - e^{-i\omega_S \rightarrow S-1t} \sigma^-}{2i} \right) \\ &= -\frac{1}{2} H_z \sigma^z - D \left( S - \frac{1}{2} \right) \sigma^z + E_0 \\ &\quad - \sqrt{2S} h_{ac} \left( \frac{e^{i\omega_S \rightarrow S-1t} \sigma^+ - e^{-i\omega_S \rightarrow S-1t} \sigma^-}{2i} \right). \end{aligned} \quad (30)$$

This two-level Hamiltonian has the same form as the Rabi Hamiltonian (8), where

$$H_z \rightarrow H_z + D(2S - 1), \quad h_{ac} \rightarrow \sqrt{2S} h_{ac}. \quad (31)$$

In the case of  $S = 1/2$ , the transformation from the model of spin operators to the two level model given by Eq. (30) is exact (it is precisely the Rabi Hamiltonian as there is no anisotropy for  $S = 1/2$ ). However, for  $S > 1/2$ , this transformation is not exact, and the expression of the two-level model by the spin operator will be discussed below. Nevertheless, this transformation constitutes a very good approximation (note that this resonance oscillation is used in the magnetic resonance (ESR), e.g., to determine energy levels separations).

To illustrate the fact that the operation  $S^\pm$  causes weak population leaking outside the specified states ( $m$  and  $m - 1$ ), let us take the example of the simplest case  $S = 1$ , where the spin operators are given by  $3 \times 3$  matrices associated with the wave vector ( $c(1)$ ,  $c(0)$ ,  $c(-1)$ ):

$$|\Psi\rangle = c(1)|1\rangle + c(0)|0\rangle + c(-1)|-1\rangle. \quad (32)$$

In our example of  $S = 1$  and  $m = 1$ ,  $\sqrt{S(S+1) - m(m-1)} = \sqrt{2}$ , and  $S^\pm$  are given by the following matrices:

$$\begin{aligned} S^- &= \sqrt{2} \begin{pmatrix} 0 & 0 & 0 \\ 1 & 0 & 0 \\ 0 & 1 & 0 \end{pmatrix}, \quad S^+ = \sqrt{2} \begin{pmatrix} 0 & 1 & 0 \\ 0 & 0 & 1 \\ 0 & 0 & 0 \end{pmatrix}, \\ |\Psi\rangle &= \begin{pmatrix} c(1) \\ c(0) \\ c(-1) \end{pmatrix}. \end{aligned} \quad (33)$$

The Hamiltonian (15) expressed in the rotating frame is written

$$\mathcal{H} = -H_z S_z - D S_z^2 - h_{ac} S_x - D S_z + E', \quad (34)$$

where  $E'$  is a constant which does not affect the dynamics. That is why we will ignore it hereafter. This Hamiltonian for  $H_z + D = 0$  is expressed by the following matrix:

$$\mathcal{H} = \begin{pmatrix} 0 & h_{ac}\sqrt{2} & 0 \\ h_{ac}\sqrt{2} & 0 & h_{ac}\sqrt{2} \\ 0 & h_{ac}\sqrt{2} & -2D \end{pmatrix}, \quad (35)$$

which operates all the states  $|1\rangle$ ,  $|0\rangle$  and  $|-1\rangle$ . Here,  $\omega_{1 \rightarrow 0} = H_z + D = 0$  while  $\omega_{0 \rightarrow -1} = H_z - D = -2D$ . When we apply only the frequency associated with the oscillations between 1 and 0, the transition between  $|0\rangle$  and  $|1\rangle$  is at resonance while the transition between  $|0\rangle$  and  $|-1\rangle$  is off-resonance and

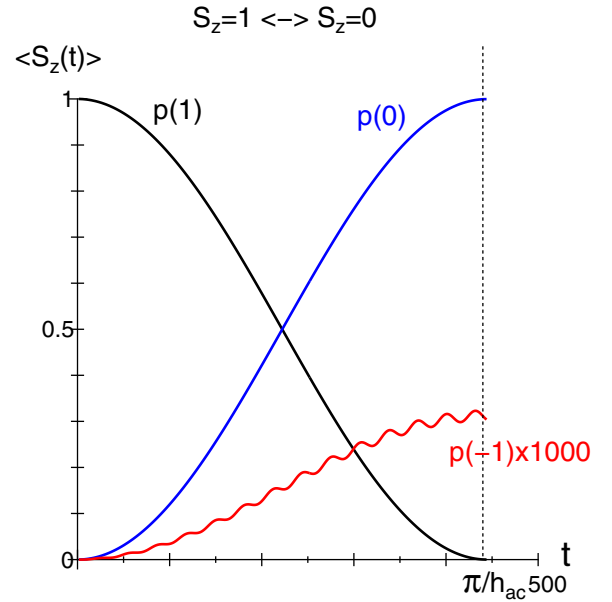


FIG. 10. The population dynamics,  $p(1)$ ,  $p(0)$  and  $p(-1) \times 1000$ .

causes a fast oscillation ( $\sim e^{2iDt}$ ) for the state  $|-1\rangle$ . Because there is the matrix element  $h_{ac}\sqrt{2}$  between  $|0\rangle$  and  $|-1\rangle$ , the small population leaks to  $|-1\rangle$  as we see in Fig. 10.

For the case of  $S = 1/2$ ,  $S_x \sin(\omega t) + S_y \cos(\omega t)$  causes the oscillations between  $1/2$  and  $-1/2$  with the resonance frequency  $\omega = \Delta E/\hbar$ . For the cases of  $S > 1/2$ , if  $D = 0$  and  $\omega = \Delta E/\hbar$ , then  $S_x \sin(\omega t) + S_y \cos(\omega t)$  causes the oscillations between  $S$  and  $-S$  where all the energy differences are the same  $\Delta E = H_z$ . However, when  $D \neq 0$ , all the energy separations are different. If we choose  $\omega = E_{S-1} - E_S$ , then  $S_x \sin(\omega t) + S_y \cos(\omega t)$  causes the oscillations between  $S$  and  $S - 1$ , but the small population leaks to  $S - 2$ .

In the case  $S = 1$ , if we choose  $\omega_{1 \rightarrow 0} = E_0 - E_1$ , then  $S_x \sin(\omega t) + S_y \cos(\omega t)$  mainly causes the oscillations between 1 and 0 but the small population leaks to  $S = -1$ . However, if we choose  $\omega_{0 \rightarrow -1} = E_{-1} - E_0$ , which is equal to  $-\omega_{1 \rightarrow 0}$ , then  $S_x \sin(\omega t) + S_y \cos(\omega t)$  causes the oscillations between 0 and  $-1$ .

To demonstrate the above-mentioned population dynamics, we, now, study the time evolution of the wave function  $\Psi(t)$  starting from  $|1\rangle$  at  $t = 0$ :

$$\Psi(t) = c_1(t)|1\rangle + c_0(t)|0\rangle + c_{-1}(t)|-1\rangle, \quad \Psi(0) = |1\rangle. \quad (36)$$

The temporal evolution of the populations of three states,

$$p(1) = |c_1(t)|^2, \quad p(0) = |c_0(t)|^2, \quad p(-1) = |c_{-1}(t)|^2, \quad (37)$$

is depicted in Fig. 10. The population  $p(-1)$  shows a nonzero population (in a proportion of about  $10^{-3}$ ) on the  $|-1\rangle$  state.

In general, when the resonance frequencies  $\omega_{m \rightarrow m-1}$  are different for every  $m$ , the operation  $X(m, m-1)$  does not seriously affect the states other than  $m$  and  $m-1$ , although it gives an off-resonance effect with fast oscillations. Thus, operations  $\{X(m, m-1)\}$  give almost independent transitions for the specified  $m$ .



### B. Example of an exact formula for transfer operation between two specified states

In this paragraph, we provide an expression to achieve an exact transfer operation between two successive

levels in systems with  $S > 1/2$ . Replacing  $\sigma^+$  ( $\sigma^-$ ) in the no-leaking Hamiltonian (30) by the operations  $|m\rangle\langle m-1|$  ( $|m-1\rangle\langle m|$ ), we get the exact transfer operation:

$$\mathcal{H} = -H_z S_z - DS_z^2 - h_{ac} \left( \frac{e^{i\omega_{S \rightarrow S-1} \sqrt{S(S+1)-m(m-1)} |m\rangle\langle m-1| t} - e^{-i\omega_{S \rightarrow S-1} \sqrt{S(S+1)-m(m-1)} |m-1\rangle\langle m| t}}{2i} \right), \quad (38)$$

which is limited to the states  $m$  and  $m-1$  (18), while the leaking out of these states persists.

Here, we consider again the example of the case  $S = 1$ , to make it simple. To eliminate leaks completely, i.e., to make  $p(-1) = 0$ , we need a more sophisticated operation. Coming back to the rotating frame, Eq. (38) is written

$$\mathcal{H} = \begin{pmatrix} 0 & \sqrt{2}h_{ac} & 0 \\ \sqrt{2}h_{ac} & 0 & 0 \\ 0 & 0 & 1 \end{pmatrix}. \quad (39)$$

This operation which is confined to the states  $|1\rangle$  and  $|0\rangle$ , can be expressed in terms of spin operator as follows:

$$S^+ S^- S^- = 2\sqrt{2} \begin{pmatrix} 0 & 1 & 0 \\ 0 & 0 & 1 \\ 0 & 0 & 0 \end{pmatrix} \begin{pmatrix} 0 & 0 & 0 \\ 1 & 0 & 0 \\ 0 & 1 & 0 \end{pmatrix} \begin{pmatrix} 0 & 0 & 0 \\ 1 & 0 & 0 \\ 0 & 1 & 0 \end{pmatrix} = 2\sqrt{2} \begin{pmatrix} 0 & 0 & 0 \\ 1 & 0 & 0 \\ 0 & 0 & 0 \end{pmatrix}, \quad (40)$$

$$|1\rangle\langle 0| + |0\rangle\langle 1| = \begin{pmatrix} 0 & 1 & 0 \\ 1 & 0 & 0 \\ 0 & 0 & 1 \end{pmatrix} = \frac{1}{2\sqrt{2}} (S^+ S^- S^- + S^+ S^+ S^-) + \frac{1}{2} (S_z^2 - S_z). \quad (41)$$

If we substitute the relations

$$S^+ = S_x + iS_y, \quad S^- = S_x - iS_y, \quad (42)$$

then we get

$$|1\rangle\langle 0| + |0\rangle\langle 1| = \mathcal{H}_{1 \leftrightarrow 0} = \frac{(S_x + iS_y)(S_x - iS_y)(S_x - iS_y) + (S_x + iS_y)(S_x + iS_y)(S_x - iS_y)}{2\sqrt{2}} + \frac{1}{2} (S_z^2 - S_z). \quad (43)$$

Contrary to the operation (18) which can be achieved by application of ac-magnetic fields, the operation  $|m\rangle\langle m-1| + |m-1\rangle\langle m|$  cannot be achieved by applying such a simple set of alternative fields, but requires to use the complex multilinear operations  $\mathcal{H}_{1 \leftrightarrow 0}$ .

To carry out the exact transfer operation (43), we need to include the multiple nonlinear operation  $h_{ac} \mathcal{H}_{1 \leftrightarrow 0}$  which consists of complicated nonlinear operations. Here, we studied the case of  $S = 1$ . But for a larger  $S$  the matrix size becomes  $(2S + 1) \times (2S + 1)$  and the expression of  $|m\rangle\langle m-1| + |m-1\rangle\langle m|$  is much more complicated. To achieve such nonlinear operations experimentally, one could try complex high order interactions such as quadrupolar interactions for the second order terms and more complicated multipolar interactions for higher products. This suggests that the exact transfer method developed above would be very difficult to achieve experimentally, if not impossible.

With leaking as small as  $10^{-3}$ , the methods based on shaped fields or  $X$  sequences, which are much simpler, are easier to implement GQAOB and look at their applications.

## VI. DYNAMICS OVER ENERGY BARRIER IN THE CLASSICAL LIMIT

As shown above, it is not possible to find a classical limit of GQAOB when they are induced by a shaped field, because

the shaped function (7),

$$f(t) = \frac{\sin(2DS t)}{\sin(Dt)},$$

has no limit when  $S \rightarrow \infty$ . In contrast, the  $X$ -method sequence resonance procedure has a limit when  $S \rightarrow \infty$ . This leads us to study the classical counterpart of GQAOB by taking an ac-field whose frequency evolves in time as predicted in the sequential case, when the spacing between levels tends towards zero, i.e., when  $S \rightarrow \infty$ .

In the classical model, the dynamics of a magnetic moment  $\mathbf{M}$  is given by the Landau-Lifshitz-Gilbert (LLG) equation [45]:

$$\frac{d}{dt} \mathbf{M} = -\gamma \mathbf{M} \times \mathbf{H}_{\text{eff}} - \alpha \mathbf{M} \times (\mathbf{M} \times \mathbf{H}_{\text{eff}}). \quad (44)$$

Equation (44) contains a dissipation term which brings any (excited) state to its ground state (at least, to its local minimum). In our study of giant oscillations, these ones are derived solely from the application of very weak nondissipative alternating fields. We do not need to have a dissipation term ( $\alpha = 0$ ) because when the spin state climbs up to the top of the barrier under the effect of such ac-fields with the appropriate helicity, it reaches to its ground state on the other side of the barrier under the effect of applied ac-fields with the opposite helicity as demonstrated in the quantum case [43]. The spin

states remain coherent, and this is why giant oscillations are observed. Note that such a spin reversal above the barrier is different from the interesting study of a classical reversal of the magnetization above the barrier, induced by a dissipative nonzero  $\alpha$ , published about ten years ago [47].

Here, we study the dynamics of the classical magnetization:

$$\mathbf{m} = \frac{\mathbf{M}}{M_S}, \quad m_x^2 + m_y^2 + m_z^2 = 1. \quad (45)$$

From Eq. (44) with  $\alpha = 0$ , the dynamics of a locally stable magnetic moment  $\mathbf{m}$  ( $m_x, m_y, m_z$ ), submitted to an effective magnetic field ( $h_x, h_y, h_z$ ) is given by

$$\begin{aligned} \frac{d}{dt}m_x &= h_y m_z - h_z m_y, \\ \frac{d}{dt}m_y &= h_z m_x - h_x m_z, \\ \frac{d}{dt}m_z &= h_x m_y - h_y m_x. \end{aligned} \quad (46)$$

As in the case of GQOAB, our magnetic moment is in a double energy well associated with a uniaxial anisotropy constant,  $K_1$  here. In the presence of a longitudinal field  $\mathbf{H} = (0, 0, H_z)$  its energy is written

$$E = -K_1 m_z^2 - H_z m_z, \quad |\mathbf{m}| = 1. \quad (47)$$

The effective field vector intervening in Eq. (46) is written

$$\mathbf{h} = \begin{pmatrix} 0 \\ 0 \\ H_z + 2K_1 m_z \end{pmatrix}. \quad (48)$$

To induce the oscillations from one well to the other one, we add a driving circular field which is, as shortly mentioned above, the limit of the ac-field applied in the sequential method when  $S \rightarrow \infty$ :

$$\mathcal{H}_{\text{circular}} = h_{\text{ac}}(\sin(\omega(t)t)m_x + \cos(\omega(t)t)m_y). \quad (49)$$

The time dependence of  $\omega(t)$  will be clarified below. It should be recalled that this circular field is on the  $xy$  plane either clockwise or anticlockwise depending on the well. The effective field in the equation of motion is written

$$\mathbf{H}_{\text{eff}} = \begin{pmatrix} h_{\text{ac}} \sin(\omega(t)t) \\ h_{\text{ac}} \cos(\omega(t)t) \\ H_z + 2K_1 m_z \end{pmatrix}. \quad (50)$$

### A. Laboratory frame

Let us study this motion in the laboratory frame. The equation of motion in the laboratory frame is given by

$$\frac{d}{dt} \begin{pmatrix} m_x \\ m_y \\ m_z \end{pmatrix} = \begin{pmatrix} h_{\text{ac}} \sin(\omega(t)t) \\ h_{\text{ac}} \cos(\omega(t)t) \\ H_z + 2K_1 m_z \end{pmatrix} \times \begin{pmatrix} m_x \\ m_y \\ m_z \end{pmatrix}. \quad (51)$$

More explicitly, it is

$$\begin{aligned} \frac{d}{dt}m_x &= h_{\text{ac}} \cos(\omega(t)t)m_z - (H_z + 2K_1 m_z)m_y, \\ \frac{d}{dt}m_y &= (H_z + 2K_1 m_z)m_x - h_{\text{ac}} \sin(\omega(t)t)m_z, \\ \frac{d}{dt}m_z &= h_{\text{ac}} \sin(\omega(t)t)m_y - h_{\text{ac}} \cos(\omega(t)t)m_x. \end{aligned} \quad (52)$$

### B. Transformation from the laboratory frame to the rotating frame

We shall now study the transformation of the equation of motion from the laboratory frame (46) to the rotating frame (see Appendix). For that, we introduce the following new variables which represent the motion in the rotating frame:

$$\begin{aligned} \tilde{m}_x &= \cos(\omega(t)t)m_x - \sin(\omega(t)t)m_y, \\ \tilde{m}_y &= \sin(\omega(t)t)m_x + \cos(\omega(t)t)m_y, \\ \tilde{m}_z &= m_z. \end{aligned} \quad (53)$$

The inverse expressions are

$$\begin{aligned} m_x &= \cos(\omega(t)t)\tilde{m}_x + \sin(\omega(t)t)\tilde{m}_y, \\ m_y &= -\sin(\omega(t)t)\tilde{m}_x + \cos(\omega(t)t)\tilde{m}_y, \\ m_z &= \tilde{m}_z, \end{aligned} \quad (54)$$

and from Eq. (46), we get

$$\begin{aligned} \sin(\omega(t)t) \frac{d}{dt}m_x + \cos(\omega(t)t) \frac{d}{dt}m_y &= \sin(\omega(t)t)h_{\text{ac}} \cos(\omega(t)t)m_z - \sin(\omega(t)t)h_z m_y \\ &\quad + \cos(\omega(t)t)h_z m_x - \cos(\omega(t)t)h_{\text{ac}} \sin(\omega(t)t)m_z \\ &= h_z(\cos(\omega(t)t)m_x - \sin(\omega(t)t)m_y) \\ &= h_z \tilde{m}_x \cos(\omega(t)t) \frac{d}{dt}m_x - \sin(\omega(t)t) \frac{d}{dt}m_y \\ &= \cos(\omega(t)t)h_{\text{ac}} \cos(\omega(t)t)m_z - \cos(\omega(t)t)h_z m_y \\ &\quad - \sin(\omega(t)t)h_z m_x + \sin(\omega(t)t)h_{\text{ac}} \sin(\omega(t)t)m_z \end{aligned} \quad (55)$$

$$= h_{\text{ac}}m_z - h_z(\cos(\omega(t)t)m_y + \sin(\omega(t)t)m_x) = h_{\text{ac}}\tilde{m}_z - h_z\tilde{m}_y \quad (56)$$

$$\begin{aligned} \frac{d}{dt}m_z &= h_{\text{ac}} \sin(\omega(t)t)(-\sin(\omega(t)t)\tilde{m}_x + \cos(\omega(t)t)\tilde{m}_y) \\ &\quad - h_{\text{ac}} \cos(\omega(t)t)(\cos(\omega(t)t)\tilde{m}_x + \sin(\omega(t)t)\tilde{m}_y) \\ &= -h_{\text{ac}}\tilde{m}_x. \end{aligned} \quad (57)$$

The time derivatives of  $\tilde{m}_x$  and  $\tilde{m}_y$  are

$$\begin{aligned} \frac{d}{dt}\tilde{m}_x &= \frac{d}{dt}(\cos(\omega(t)t)m_x - \sin(\omega(t)t)m_y) \\ &= \frac{d \cos(\omega(t)t)}{dt}m_x - \frac{d \sin(\omega(t)t)}{dt}m_y \\ &\quad + \cos(\omega(t)t) \frac{d}{dt}m_x - \sin(\omega(t)t) \frac{d}{dt}m_y \end{aligned}$$

$$\begin{aligned}
 &= \frac{d}{dt}(\omega(t)t)(-\sin(\omega(t)t)m_x - \cos(\omega(t)t)m_y) \\
 &\quad + \cos(\omega(t)t)\frac{d}{dt}m_x - \sin(\omega(t)t)\frac{d}{dt}m_y \\
 &= -\frac{d}{dt}(\omega(t)t)\tilde{m}_y + \cos(\omega(t)t)\frac{d}{dt}m_x - \sin(\omega(t)t)\frac{d}{dt}m_y \\
 &= -\frac{d}{dt}(\omega(t)t)\tilde{m}_y + h_{ac}m_z - h_z\tilde{m}_y \\
 &= -\left(\frac{d}{dt}(\omega(t)t) + h_z\right) + h_{ac}m_z \quad (58) \\
 \frac{d}{dt}\tilde{m}_y &= \frac{d}{dt}(\sin(\omega(t)t)m_x + \cos(\omega(t)t)m_y) \\
 &= \frac{d \sin(\omega(t)t)}{dt}m_x + \frac{d \cos(\omega(t)t)}{dt}m_y \\
 &\quad + \sin(\omega(t)t)\frac{d}{dt}m_x + \cos(\omega(t)t)\frac{d}{dt}m_y \\
 &= \frac{d}{dt}(\omega(t)t)(\cos(\omega(t)t)m_x - \sin(\omega(t)t)m_y) \\
 &\quad + \sin(\omega(t)t)\frac{d}{dt}m_x + \cos(\omega(t)t)\frac{d}{dt}m_y \\
 &= \frac{d}{dt}(\omega(t)t)\tilde{m}_x + h_z\tilde{m}_x = \left(\frac{d}{dt}(\omega(t)t) + h_z\right)\tilde{m}_x. \quad (59)
 \end{aligned}$$

We then set the following condition, which is the limit of the X sequence Eq. (20) when the spin  $S \rightarrow \infty$ :

$$\frac{d}{dt}(\omega(t)t) + h_z = 0, \quad h_z = H_z + 2K_1m_z. \quad (60)$$

Using this condition, the equations of motion (57), (58), and (59) become

$$\begin{aligned}
 \frac{d}{dt}\tilde{m}_x &= h_{ac}\tilde{m}_z, \\
 \frac{d}{dt}\tilde{m}_y &= 0, \\
 \frac{d}{dt}\tilde{m}_z &= -h_{ac}\tilde{m}_x. \quad (61)
 \end{aligned}$$

The condition for instantaneous resonance is obtained from Eq. (60):

$$\frac{d}{dt}(\omega(t)t) = \omega(t) + \frac{d\omega(t)}{dt}t = -(H_z + 2K_1m_z). \quad (62)$$

To satisfy Eq. (62),  $\omega(t)$  is given by

$$\begin{aligned}
 \omega(t)t &= -\int_0^t (H_z + 2K_1m_z(t'))dt' \rightarrow \omega(t) \\
 &= -\frac{1}{t} \int_0^t (H_z + 2K_1m_z(t'))dt'. \quad (63)
 \end{aligned}$$

Thus, the condition is given by

$$\begin{aligned}
 \omega(t) &= -H_z - 2K_1\tilde{m}_z(t), \\
 \tilde{m}_z(t) &= \frac{1}{t} \int_0^t m_z(t')dt', \quad (t > 0), \quad (64)
 \end{aligned}$$

and  $\omega(0) = -(H_z + 2K_1m_z(0))$ .

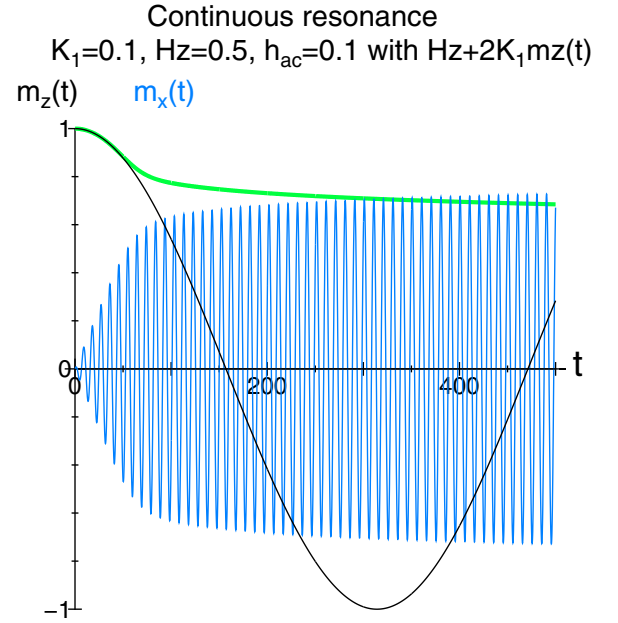


FIG. 11.  $m_z(t)$  (bold green curve) and  $m_x(t)$  (thin blue oscillations) for  $K_1 = 0.1$ ,  $H_z = 0.5$ ,  $h_{ac} = 0.01$  with the continuous resonance  $\omega(t) = 2K_1m_z(t) + H_z$ . The thin black curve is  $m_z(t)$  for  $K_1 = 0$  (usual Rabi oscillations).

### C. Numerical confirmation of the continuous resonance

Equation (64) constitutes the most logical choice for  $\omega(t)$ . However, before starting with this expression, which is not easy to be achieved experimentally, we performed calculations with simpler choices of  $\omega(t)$ .

#### 1. With the approximate resonance condition

First, we performed numerical simulation with the approximate resonance condition:

$$\omega(t) = -(H_z + 2K_1m_z(t)). \quad (65)$$

In Fig. 11, we show an example of  $S_z(t)/S$  calculated under this choice (65). There, we find  $m_z(t)$  follows the Rabi oscillation ( $K_1 = 0$ ) in the initial short term, but it quickly deviates from this trajectory. The  $x$  and  $y$  components rotate around the  $z$  axis rapidly with the frequency  $\omega(t)$ . The spin does not reverse, and we see that we cannot achieve giant oscillations with this choice.

#### 2. With the correct resonance condition (64)

Next, we performed numerical simulation with the correct resonance condition (62):

$$\omega(t) = -\left(H_z + \frac{2K_1}{t} \int_0^t m_z(t')dt'\right), \quad (t > 0).$$

In this case, the angular momentum  $m(t)$  depends on the complex history of the magnetic moment, which should be difficult to achieve experimentally. This is clearly not the case for simulations which can be performed after simple integration.

In Fig. 12, we show an example of giant classical oscillations above the barrier (GCOAB) where the magnetization perfectly reverses. Interestingly such GCOAB with the

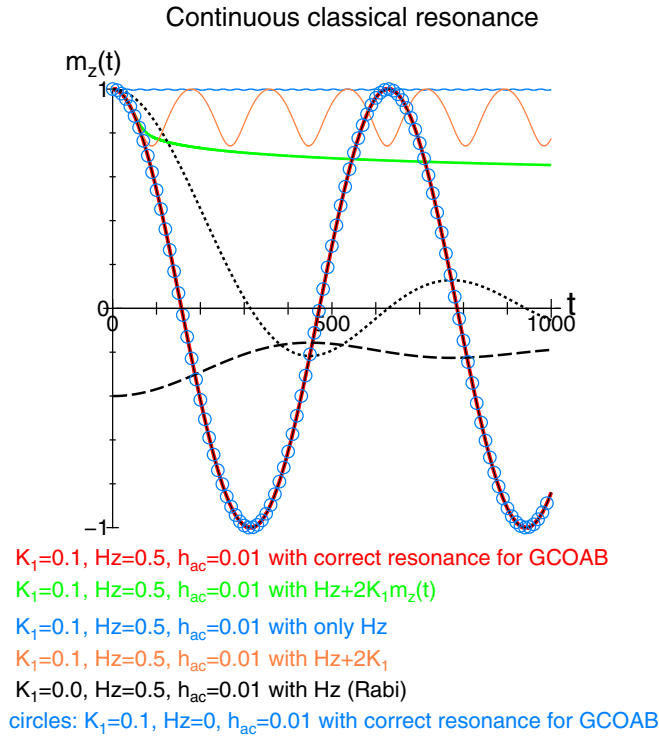


FIG. 12.  $m_z(t)$  in the laboratory frame (bold red curve) for  $K_1=0.1$ ,  $H_z=0.5$ ,  $h_{ac}=0.01$ , giving the GCOAB with the correct continuous resonance (62). The thin black curve is  $m_z(t)$  for  $K_1=0$  (usual Rabi oscillations) is not really visible because it perfectly superimposes the red one. The circles show result with  $H_z=0$ , which coincides perfectly with those obtained with nonzero  $H_z$ . The orange curve shows  $m_x(t)$  for the nonoptimal choice  $\omega(t) = -(H_z + 2K_1)$ , and the blue curve  $\omega(t) = -H_z$ . The quantities,  $\bar{m}_z(t)$  in Eq. (64) and  $\omega(t)$ , are also plotted by short-dotted and long-dotted curves, respectively.

example  $K_1=0.1$  perfectly coincide with the Rabi oscillations calculated with  $K_1=0$  and the same value of  $H_z$ . This shows that the application of the sweeping ac-field corresponding to the correct resonance condition indeed causes the giant classical oscillations over the energy barrier. It is also interesting to note that the calculation with  $H_z=0$  coincides perfectly with those obtained with nonzero  $H_z$  (Fig. 12). This result, checked for other values of  $H_z$ , shows that, as the GQOAB, GCOAB are field-independent, as long as this field is not time-dependent.

To compare, we have also calculated the cases relative to other choices (i) for  $\omega(t) = H_z + 2D$  (orange curve) and (ii) for  $\omega(t) = H_z$  (blue curve). In both cases of the magnetization does not reverse but stays around  $m_z(t) \simeq 1$ .

In Fig. 12, we also plot the time-averaged magnetic moment  $\bar{m}_z(t)$  (short-dotted curve) and  $\omega(t)$  for GCOAB (long-dotted curve) given in Eq. (64):

$$\bar{m}_z(t) = \frac{1}{t} \int_0^t m_z(t') dt', \quad (t > 0),$$

which changes smoothly. In spite of the relative complexity of Eq. (64), such a smooth variation suggests relatively easy experimental realization with the application of an adapted shaped field.

#### D. Explicit formula for $\bar{m}_z$

Using the motion of the magnetic moments given by Eq. (61),  $\bar{m}_z(t)$  is simply sinusoidal. The  $z$ -component in the laboratory and the rotation frames are the same and are given by

$$m_z(t) = \bar{m}_z = \cos(h_{ac}t), \quad \bar{m}_x = \sin(h_{ac}t). \quad (66)$$

Using this, the time-averaged magnetic moment  $\bar{m}_z$  in Eq. (64) is explicitly given as

$$\frac{1}{t} \int_0^t m_z(t') dt' = \frac{1}{th_{ac}} \sin(h_{ac}t), \quad (67)$$

and  $\omega(t)$  (62) is given by

$$\omega(t) = -\left(H_z + \frac{2K_1}{th_{ac}} \sin(h_{ac}t)\right), \quad (t > 0). \quad (68)$$

In this case, the applied frequency  $\omega(t)$  (62) approaches to  $-H_z$  over time as  $1/t$ . Note that (62) shows that  $H_z$  simply gives a constant shift to the time-dependent frequency, explaining why GCOAB are independent of  $H_z$  (Fig. 12). Besides, using Eqs. (63) and (67) we get

$$\omega(t)t = -H_z t - \frac{2K_1}{h_{ac}} \sin(h_{ac}t). \quad (69)$$

With this  $\omega(t)t$ , the driving ac-field in the laboratory frame (51), limited to the two in-plane components, is written

$$\begin{aligned} & h_{ac}(m_x \sin(\omega(t)t) + m_y \cos(\omega(t)t)) \\ &= h_{ac} \left( m_x \sin \left( -H_z t - \frac{2K_1}{h_{ac}} \sin(h_{ac}t) \right) \right. \\ & \quad \left. + m_y \cos \left( -H_z t - \frac{2K_1}{h_{ac}} \sin(h_{ac}t) \right) \right), \quad (70) \end{aligned}$$

which is a periodic function with the period  $2\pi/h_{ac}$ , and it should be regarded as a time-dependent phase shift:

$$\phi(t) = -\frac{2K_1}{h_{ac}} \sin(h_{ac}t). \quad (71)$$

In the case of no anisotropy ( $K_1=0$ ) the driving ac-field is just for the usual Rabi oscillations, i.e.,  $\omega = -H_z$ . This time-dependent phase shift gives the correction to the case without the anisotropy. Such an applied ac-field is regarded as the shaped field for GCOAB.

Despite its apparent complexity, the numerical plot of Eq. (70) shows a fairly simple evolution that should easily be represented by a fit to a simple function, used as a shaped field.

## VII. SUMMARY AND DISCUSSION

In this paper, we studied in detail the dependencies of GQOAB [43] on the anisotropy constant  $D$  and the applied ac-fields  $h_{ac}$ . When  $D$  becomes small, the resonance frequencies associated with the different continuous pairs of states become close to each other. In the limit of  $D=0$ , the usual Rabi oscillations occur, but with a  $2S$  times shorter period. In between, when  $D$  is not zero but very small, the dynamics becomes complex. For relatively large values of  $h_{ac}$ , GQOAB show a bumpy shape as we reported in the previous work [43],

while for small values of  $h_{ac}$ , the period becomes close to a simple sinusoid. However, it is essentially different from the usual Rabi oscillations, because oscillations above the barrier are impossible with simple Rabi oscillations. Note that, as a consequence,  $s_f$  (length of the magnetization vector) changes in time (quantum regime), while it is constant  $s_f = S^2$  in the usual Rabi oscillations and also in the case of GCOAB (classical regime). This observation specifies the quantum character of GQOAB and the classical one of Rabi oscillations.

We studied the transfer operation between neighboring levels. The simplest one consists in applying a  $\pi$ -pulse at resonance, the same as usually used in ESR type measurements. We pointed out that this operation is not exact for the transfer between two specified levels and induces weak nonresonant transfers ( $\sim 10^{-3}$ ) to other states which are presumably the cause of the GQOAB beatings observed at long times.

As an alternative protocol for reversing the magnetization above the barrier, we have also proposed the idea of applying  $\pi$  pulses corresponding to all consecutive state separations. However, this idea is difficult to apply both numerically and experimentally, as it requires very precise pulse durations.

Furthermore, with the aim of eliminating almost all the leakings to neighboring states, we derived an exact transfer operation between specified levels, requiring nonlinear products of spin operators which cannot be realized by manipulation of external magnetic field. Unfortunately, such a nonlinear process is too complicated to be implemented experimentally. We conclude that the shaped field procedure is the most efficient one to get good GQOAB. In the second part of this paper, we studied the possibilities of obtaining giant classical oscillations above the barrier. We pointed out that this is not possible if one starts from shaped fields when  $S \rightarrow \infty$ . However, this is quite possible by applying an ac magnetic field whose frequency is time-dependent and given by Eq. (64).

The dynamics of the QOAB studied in this article and in our previous paper [43] must inevitably be perturbed by dissipation and decoherence effects [48,49]. As far as dissipation and decoherence effects are concerned, they can be related to studies of the decay of Rabi oscillations. Indeed, these oscillations have recently been observed down to time scales of the order of ms [28,50,51]. Although there are several types of decay mechanism, these coherence times of Rabi oscillations indicate that spin reversal by the GQOAB mechanism, which only requires coherence over a half-period of the Rabi oscillation, should also be at least of the order of a millisecond.

Furthermore, in single-spin systems, such as molecular magnets or highly diluted rare-earth alloys, the sizes of the spins or of the total angular momentum, are not so large, and

so is the number of frequencies to be applied. In these cases, the use of the shaped field  $f(t)$  (7) is perfectly feasible. We are working on an experimental realization in a molecular magnet [52].

As far as classical giant oscillations (GCOAB) are concerned, they could be tested on single-domain nanoparticles, which form an important part of mesoscopic systems [9–22]. Indeed, the size of the spin per particle can be modulated by the size of the nanoparticle, offering the possibility of obtaining separations between levels as small as desired.

Although temporal control of frequency is difficult, adjusted magnetization  $\tilde{m}_z(t)$  given in Eq. (64) and  $\omega(t)$  change smoothly as shown in Fig. 12. Therefore an approximate form of  $\omega(t)$  could, in practice, help reverse the magnetization, which will be left for future study. In such cases, the application of an alternating field with a continuously varying frequency, as demonstrated above, should lead to the observation of GCOABs.

## ACKNOWLEDGMENTS

The authors thank E. Chudnovsky for bringing Ref. [47] to their attention. This work was supported by the Elements Strategy Initiative Center for Magnetic Materials (ESICMM) (Grant No. 12016013) funded by the Ministry of Education, Culture, Sports, Science and Technology (MEXT) of Japan, and was partially supported by Grants-in-Aid for Scientific Research C (Grants No. 18K03444 and No. 20K03809) from MEXT.

## APPENDIX: GENERAL FORMULA FOR MOTION IN ROTATING FRAME

In the rotating frame with an angular velocity vector  $\tilde{\omega}(t)$  which is a vector along the axis of the rotation (upward direction for counterclockwise rotation) and its strength  $\tilde{\omega} = |\tilde{\omega}(t)|$ , a change of vector in the laboratory frame is transformed as

$$\frac{d}{dt}\mathbf{A}(t) \rightarrow \frac{d'}{dt}\mathbf{A}(t) + \tilde{\omega}(t) \times \mathbf{A}(t), \quad (\text{A1})$$

where  $d'/dt$  is the derivative in the rotation frame.

If the time dependence of the frame is given by  $\Omega(t)$ , then

$$\tilde{\omega}(t) = \frac{d}{dt}\Omega(t). \quad (\text{A2})$$

When we express  $\Omega(t) = \omega(t)t$ ,  $\tilde{\omega}(t)$  is given by

$$\tilde{\omega}(t) = \omega(t) + \frac{d\omega(t)}{dt}t. \quad (\text{A3})$$

- 
- [1] C. Cohen-Tanoudji, B. Diu, and F. Lalo, *Quantum Mechanics: Basic Concepts, Tools, and Applications* (Blackwell Verlag, Berlin, 2019); S. Miyashita, *J. Comput. Theoret. Nanosci.* **8**, 1919 (2011).  
 [2] H. Kramers, *Physica* **7**, 284 (1940).  
 [3] P. W. Anderson, *Rev. Mod. Phys.* **38**, 298 (1966).  
 [4] J. S. Langer, *Ann. Phys.* **41**, 108 (1967); **54**, 258 (1969).  
 [5] I. Affleck, *Phys. Rev. Lett.* **46**, 388 (1981).

- [6] C. G. Callan and S. Coleman, *Phys. Rev. D* **16**, 1762 (1977); S. Coleman, *Aspects of Symmetry* (Cambridge University Press, Cambridge, UK, 1985).  
 [7] S. Miyashita, *Collapse of Metastability* (Springer-Nature, Singapore, 2022).  
 [8] T. Hatomura, B. Barbara and S. Miyashita, *Phys. Rev. Lett.* **116**, 037203 (2016); *Phys. Rev. B* **96**, 134309 (2017).

- [9] Y. Imry, *Introduction to Mesoscopic Physics (Mesoscopic Physics and Nanotechnology)*, 2nd ed. (Oxford University Press, New York, NY, 2008); with this reference, also J. Ankerhold, *Quantum Tunneling in Complex Systems: The Semi-classical Approach* (Springer, Berlin, Heidelberg, 2006); S. A. Owerre and M. B. Paranjape, *Phys. Rep.* **546**, 1 (2015);
- [10] L. Gunther and B. Barbara, Editors and directors of publication. *Quantum Tunneling of Magnetization* (Springer, Berlin, 1995); *NATO Workshop on Quantum Tunneling of Magnetization*, Chichilianne, France.
- [11] P. C. E. Stamp, E. Chudnovsky, and B. Barbara, *Int. J. Mod. Phys. B* **06**, 1355 (1992).
- [12] B. Barbara, in *Proceedings of the 2nd International Symposium on Magnetic Anisotropy and Coercivity in Rare-earth Transition Metal Alloys*, edited by K. J. Strnat (University of Dayton, School of Engineering, 1978), Vol. 37.
- [13] T. Egami, *Phys. Status Solidi* **20**, 157 (1973); **57**, 211 (1973).
- [14] M. Uehara and B. Barbara, *J. Phys. France* **47**, 235 (1986).
- [15] B. Barbara, P. C. E. Stamp, and M. Uehara, *Journal de Physique Colloques* **49**, C8-529 (1988).
- [16] B. Barbara, L. C. Sampaio, J. E. Wegrowe, B. A. Ratnam, A. March, C. Paulsen, M. A. Novak, J. L. Tholence, M. Uehara, and D. Fruchart, *J. Appl. Phys.* **73**, 6703 (1993).
- [17] B. Barbara, W. Wernsdorfer, E. Bonet Orozco, K. Hasselbach, A. Benoit, D. Mailly, N. Demoncey, H. Pascard, L. Francois, N. Duxin, and M. P. Pileni, *MRS Proc.* **475**, 265 (1997).
- [18] W. Wernsdorfer, E. Bonet Orozco, K. Hasselbach, A. Benoit, D. Mailly, O. Kubo H. Nakano, and B. Barbara, *Phys. Rev. Lett.* **79**, 4014 (1997).
- [19] B. Barbara, W. Wernsdorfer, L. C. Sampaio, J. G. Park, C. Paulsen, M. A. Novak, R. Ferré, D. Mailly, R. Sessoli, A. Caneschi, K. Hasselbach, A. Benoit, and L. Thomas, *J. Magn. Magn. Mater.* **140-144**, 1825 (1995).
- [20] B. Barbara, *Philos. Trans. R. Soc. London A* **370**, 4487 (2012).
- [21] B. Barbara and E. M. Chudnovsky, *Phys. Lett. A* **145**, 205 (1990).
- [22] L. Thomas, F. Lioni, R. Ballou, D. Gatteschi, R. Sessoli, and B. Barbara, *Nature (London)* **383**, 145 (1996).
- [23] J. R. Friedman, M. P. Sarachik, J. Tejada, and R. Ziolo, *Phys. Rev. Lett.* **76**, 3830 (1996).
- [24] J. A. A. J. Perenboom, J. S. Brooks, S. Hill, T. Hathaway, and N. S. Dalal, *Phys. Rev. B* **58**, 330 (1998).
- [25] W. Wernsdorfer, R. Sessoli, A. Caneschi, D. Gatteschi, A. Cornia, and D. Mailly, *J. Appl. Phys.* **87**, 5481 (2000).
- [26] E. del Barco, J. M. Hernandez, J. Tejada, N. Biskup, R. Achey, I. Rutel, N. Dalal, and J. Brooks, *Phys. Rev. B* **62**, 3018 (2000).
- [27] D. Gatteschi, R. Sessoli, and J. Villain, *Molecular Nanomagnets* (Oxford University Press, Oxford, UK, 2006).
- [28] S. Bertaina, S. Gambarelli, A. Tkachuk, I. N. Kurkin, B. Malkin, A. Stepanov and B. Barbara, *Nat. Nanotechnol.* **2**, 39 (2007); S. Bertaina, S. Gambarelli, T. Mitra, B. Tsukerblat, A. Müller, and B. Barbara, *Nature (London)* **453**, 203 (2008).
- [29] R. Giraud, W. Wernsdorfer, A. M. Tkachuk, D. Mailly, and B. Barbara, *Phys. Rev. Lett.* **87**, 057203 (2001).
- [30] S. Carretta, D. Zueco, A. Chiesa, A. Gomez-Leon, and F. Luis, *Appl. Phys. Lett.* **118**, 240501 (2021).
- [31] G. Burkard, T. D. Ladd, A. Pan, J. M. Nichol, and J. R. Petta, *Rev. Mod. Phys.* **95**, 025003 (2023); R. Cebulka and E. del Barco, *Rev. Sci. Instrum.* **90**, 085106 (2019).
- [32] C. Bonizzoni, A. Ghirri, K. Bader, J. van Slageren, M. Perfetti, L. Sorace, Y. Lan, O. Fuhr, M. Ruben, and M. Affronte, *Dalton Trans.* **45**, 16596 (2016).
- [33] C. Bonizzoni, A. Ghirri, F. Santanni, M. Atzori, L. Sorace, R. Sessoli, and M. Affronte, *npj Quantum Inf.* **6**, 68 (2020).
- [34] I. Gimeno, A. Urtizberea, J. Roman-Roche, D. Zueco, A. Camon, P. J. Alonso, O. Roubeau, and F. Luis, *Chem. Sci.* **12**, 5621 (2021).
- [35] M. D. Jenkins, Y. Duan, B. Diosdado, J. J. Garcia-Ripoll, A. Gaita-Arino, C. Gimenez-Saiz, P. J. Alonso, E. Coronado, and F. Luis, *Phys. Rev. B* **95**, 064423 (2017).
- [36] V. Rollano, M. C. de Ory, C. D. Buch, M. Rubin-Osanz, D. Zueco, C. Sanchez-Azqueta, A. Chiesa, D. Granados, S. Carretta, A. Gomez, S. Piligkos, and F. Luis, *Commun. Phys.* **5**, 246 (2022).
- [37] G. Franco-Rivera, J. Cochran, L. Chen, S. Bertaina, and I. Chiorescu, *Phys. Rev. Appl.* **18**, 014054.
- [38] M. Chizzini, L. Crippa, L. Zaccardi, E. Macaluso, S. Carretta, A. Chiesa, and P. Santini, *Phys. Chem. Chem. Phys.* **24**, 20030 (2022).
- [39] S. Chicco, A. Chiesa, G. Allodi, E. Garlatti, M. Atzori, L. Sorace, R. De Renzi, R. Sessoli, and S. Carretta, *Chem. Sci.* **12**, 12046 (2021).
- [40] E. Macaluso, M. Rubin, D. Aguilia, A. Chiesa, Leoni A. Barrios, J. I. Martinez, P. J. Alonso, O. Roubeau, F. Luis, G. Aromi, and S. Carretta, *Chem. Sci.* **11**, 10337 (2020).
- [41] A. Castro, A. Garcia Carrizo, S. Roca, D. Zueco, and F. Luis, *Phys. Rev. Appl.* **17**, 064028 (2022).
- [42] C. Godfrin, A. Ferhat, R. Ballou, S. Klyatskaya, M. Ruben, W. Wernsdorfer, and F. Balestro, *Phys. Rev. Lett.* **119**, 187702 (2017).
- [43] S. Miyashita and B. Barbara, *Phys. Rev. Lett.* **131**, 066701 (2023).
- [44] P. E. Spindler, P. Schöps, W. Kallies, S. J. Glaser, and T. F. Prisner, *J. Magn. Reson.* **280**, 30 (2017).
- [45] L. D. Landau and L. M. Lifshitz, *Physik. Zeits. Sowjetunion* **8**, 153 (1935); T. L. Gilbert, *IEEE Trans. Mag.* **40**, 3443 (2004).
- [46] L. Sorace, W. Wernsdorfer, C. Thirion, A.-L. Barra, M. Pacchioni, D. Mailly, and B. Barbara, *Phys. Rev. B* **68**, 220407(R) (2003).
- [47] L. Cai, D. A. Garanin, and E. M. Chudonovsky, *Phys. Rev. B* **87**, 024418 (2013).
- [48] A. J. Leggett, S. Chakravarty, A. T. Dorsey, M. P. A. Fisher, A. Garg, and W. Zwerger, *Rev. Mod. Phys.* **59**, 1 (1987); A. O. Caldeira and A. J. Leggett, *Phys. Rev. Lett.* **46**, 211 (1981); *Ann. Phys.* **149**, 374 (1983); *Phys. Rev. A* **31**, 1059 (1985).
- [49] N. V. Prokof'ev and P. C. E. Stamp, *Rep. Prog. Phys.* **63**, 669 (2000).
- [50] E. I. Baibekov, M. R. Gafurov, D. G. Zverev, I. N. Kurkin, A. A. Rodionov, B. Z. Malkin, and B. Barbara, *Phys. Rev. B* **95**, 064427 (2017).
- [51] H. De Raedt, S. Miyashita, K. Michielsen, H. Vezin, S. Bertaina, and I. Chiorescu, *Eur. Phys. J. B* **95**, 158 (2022).
- [52] S. Gambarelli *et al.* (unpublished).